



# Chloctanspirones A and B, novel chlorinated polyketides with an unprecedented skeleton, from marine sediment derived fungus *Penicillium terrestre*

Dehai Li<sup>a,b</sup>, Li Chen<sup>c</sup>, Tianjiao Zhu<sup>a,b</sup>, Tibor Kurtán<sup>d,\*</sup>, Attila Mándi<sup>d</sup>, Zhimin Zhao<sup>a,b</sup>, Jing Li<sup>a,b,\*</sup>, Qianqun Gu<sup>a,b,\*</sup>

<sup>a</sup> Key Laboratory of Marine Drugs, Chinese Ministry of Education, Ocean University of China, 5 Yushan Road, Qingdao, Shandong 266003, PR China

<sup>b</sup> School of Medicine and Pharmacy, Ocean University of China, 5 Yushan Road, Qingdao, Shandong 266003, PR China

<sup>c</sup> Institute of Biomedical and Pharmaceutical Technology, Fuzhou University, 2 Xueyuan Road, Fuzhou, Fujian 350002, PR China

<sup>d</sup> Department of Organic Chemistry, University of Debrecen, POB 20, 4010 Debrecen, Hungary

## ARTICLE INFO

### Article history:

Received 1 June 2011

Received in revised form 29 July 2011

Accepted 16 August 2011

Available online 22 August 2011

### Keywords:

Sorbicillinoids

Marine derived fungus

*Penicillium terrestre*

## ABSTRACT

Two novel chlorinated sorbicillinoids named chloctanspirones A (**1**) and B (**2**), possessing an unprecedented bicyclo[2.2.2]octane-2-spiro cyclohexane skeleton, together with their quasi-precursors terrestrols K (**3**) and L (**4**), two additional new chlorinated compounds, were isolated from a marine sediment derived fungus *Penicillium terrestre*. Their structures including absolute stereochemistries were elucidated by analysis of NMR, MS data, and TDDFT CD calculations. The cytotoxic effects of **1–4** were preliminarily evaluated in HL-60 and A-549 cells. Compound **1** was active against both HL-60 and A-549 cells with IC<sub>50</sub>s 9.2 and 39.7 μM, respectively, while **2** showed weaker activity only against HL-60 cells (IC<sub>50</sub> 37.8 μM).

© 2011 Elsevier Ltd. All rights reserved.

## 1. Introduction

Marine derived microorganisms especially fungi have the potential to produce compounds with high chemical diversity.<sup>1</sup> Some of them often produce different types of secondary metabolites just by the alteration of easily accessible cultivation parameters, which was termed OSMAC (One Strain-MANY Compounds) approach, proved to be a very successful strategy for finding novel secondary metabolites.<sup>2</sup> In the course of our continuous search for new bioactive secondary metabolites from marine derived fungi, several new sorbicillinoids have been isolated from the fungus strain *Penicillium terrestre*.<sup>3</sup> Different culture conditions guided by the OSMAC approach dramatically changed the secondary metabolites of this strain which led to the isolation of thirteen cytotoxic gentisyl alcohol derivatives.<sup>4</sup> Interestingly, most of them were chlorinated, which revealed that alternative culture conditions may have activated the halogenase enzyme and led to more halogenated compounds. Further investigation of the extract again resulted in the isolation of two novel chlorinated sorbicillinoids named chloctanspirones A (**1**) and B (**2**), (Fig. 1) possessing an unprecedented bicyclo[2.2.2]octane-2-spiro cyclohexane skeleton. In addition,

their quasi-precursors terrestrols K (**3**) and L (**4**), (Fig. 1) two additional new chlorinated compounds, were also isolated parallel. Up to now, chloctanspirones A (**1**) and B (**2**) are the first examples of sorbicillinoids containing spiro cyclohexane moieties and chlorinated sorbicillinoids have not been reported yet. This paper describes the isolation and structural elucidation of the new compounds together with a tentative biosynthetic route of **1** and **2**.

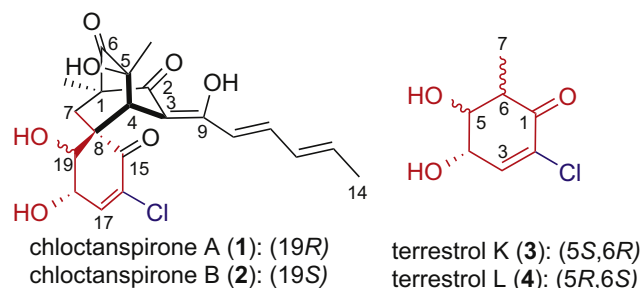


Fig. 1. Structures of compounds **1–4**.

## 2. Results and discussion

The fungus was cultured and extracted as disclosed in the previous report.<sup>4</sup> The active crude extract was fractionated by using silica gel column chromatography followed by chromatography on

\* Corresponding authors. Tel.: +86 532 82032065; fax: +86 532 82033054; e-mail addresses: [kurtant@tigris.klte.hu](mailto:kurtant@tigris.klte.hu) (T. Kurtán), [ljilic@163.com](mailto:ljilic@163.com) (J. Li), [guqianq@ouc.edu.cn](mailto:guqianq@ouc.edu.cn) (Q. Gu).

Sephadex LH20 and finally purified by preparative HPLC column to give **1** (13.6 mg), **2** (13.1 mg), **3** (10.3 mg), and **4** (4.9 mg).

Chloctanspirone A (**1**) was obtained as a yellow powder. The negative LRESIMS exhibited a characteristic chlorinated quasi-molecular ion peak cluster at  $m/z$  421/423 (3:1) ( $[M-H]^-$ ), and its molecular formula was determined as  $C_{21}H_{23}O_7Cl$  by HRESIMS, which was in agreement with its  $^1H$  and  $^{13}C$  NMR data. 1D NMR data showed the presence of three  $sp^3$  hybridized methine groups, two of them attached to oxygen, five  $sp^2$  hybridized methine groups, one methylene group, one allylic methyl group, two methyl groups attached to quaternary carbons, and nine quaternary carbons.

The 1,3-pentadienyl moiety of the sorbyl group from C-10 to C-14 was indicated by the characteristic proton chemical shifts<sup>3,5</sup> at  $\delta_H$  6.41, 7.12, 6.32, 6.21, and 1.84 ppm, which were also confirmed by the COSY and HMBC spectra (Table 1). The *E* configurations of the two double bonds in the sorbyl residue was determined via the large coupling constants ( $^3J_{12,13}=15.1$  Hz,  $^3J_{10,11}=14.6$  Hz) observed. The presence of bicyclo[2.2.2]octane moiety was suggested by the comparison of 1D NMR data of **1** with those of known sorbicillin derivatives<sup>5,6</sup> and confirmed by the HMBC correlations from H-4 ( $\delta_H=3.49$  ppm) to C-2 ( $\delta_C=198.3$  ppm), C-3 ( $\delta_C=109.3$  ppm), C-5 ( $\delta_C=74.8$  ppm), C-6 ( $\delta_C=210.2$  ppm), C-7 ( $\delta_C=38.0$  ppm), and C-8 ( $\delta_C=57.6$  ppm), and from H-7 ( $\delta_H=1.75$ , 2.57 ppm) to C-1 ( $\delta_C=59.4$  ppm), C-2, C-4 ( $\delta_C=45.2$  ppm), C-6, and C-8. The positions of  $CH_3$ -1,  $CH_3$ -5, and OH-5 were assigned according to the HMBC correlations between  $CH_3$ -1 ( $\delta_H=1.10$  ppm) and C-1, C-2, C-6, and C-7, between  $CH_3$ -5 ( $\delta_H=1.07$  ppm) and C-4, C-5 and C-6, and between OH-5 ( $\delta_H=6.37$  ppm) and C-4, C-5, and C-6. The connection of C-3 and C-10 via C-9 was deduced from HMBC correlations of OH-9 to C-3 and C-9, and of H-10 to C-3 and C-9. The dihydroxycyclohexenone moiety was established on the basis of COSY correlations (OH-18/H-18/H-19/OH-19) and HMBC correlations between OH-18 and C-17, C-18 and C-19, between H-17 and C-15, C-16 and C-19, between OH-19 and C-8, and between H-19 and C-15. With  $C_{21}H_{23}O_7$  accounted for, the planar structure was determined

by introducing the chlorine atom to C-16 in accordance with the molecular formula and chemical shift of C-16 ( $\delta_C=128.3$  ppm). Selective gradient NOE data and analysis of  $^3J_{H,H}$  proton coupling constants were used to determine the relative configuration. The bridged ring system is only possible if H-4 and  $CH_3$ -1 are oriented equatorially. NOE enhancement of OH-5 was observed by irradiation of H-19 ( $\delta_H=4.66$  ppm), showing that OH-5 was oriented toward the cyclohexene and C-19 was *cis* to C-5. With these findings, the relative configuration of this part of the molecule was designated as (1*R*\*,4*S*\*,5*S*\*,8*R*\*). The NOE enhancements for H-4 and H-18 upon irradiation of the H-19 resonance, as well as enhancements for H-4 and H-19 upon irradiation of the H-18 resonance ( $\delta_H=5.03$  ppm) indicated the H-18 and H-19 to be located on the same side of cyclohexene and to be oriented toward the sorbyl side chain. The *cis* configuration of H-18 and H-19 was also supported by the small coupling constant measured for  $^3J_{18,19}$  (3.2 Hz). Based on these evidences, the relative configuration of **1** was proposed as (1*R*\*,4*S*\*,5*S*\*,8*R*\*,18*S*\*,19*R*\*). The interatomic distances of protons in the lowest-energy conformer were all in agreement with the observed NOE effects (Fig. 2b). The CD spectrum of **1** showed intense positive Cotton Effects (CEs) at 356 and 248 nm and negative ones at 306 and 219 nm. In order to determine the absolute configuration, the TDDFT CD calculations were carried out on the computed solution conformers. An MMFF conformational search followed by DFT optimization afforded three slightly different conformers (65.4, 27.2, and 6.9% populations) above 0.5% population (Fig. 3). In all the three conformers, the OH-19 had axial and the OH-18 had equatorial orientation in agreement with the measured coupling constants, and OH-5 and OH-9 were hydrogen bonded to carbonyl groups. Then the CD spectra of each conformer were calculated by various functionals (B3LYP, BH&HLYP, PBE0) and TZVP basis set. The Boltzmann-weighted CD spectra of the (1*R*,4*S*,5*S*,8*R*,18*S*,19*R*)-enantiomer reproduced well the experimental CD curve with PBE0/TZVP giving the best agreement (Fig. 4). Thus the absolute configuration of **1** was determined unambiguously as (+)-(1*R*,4*S*,5*S*,8*R*,18*S*,19*R*).

**Table 1**  
NMR data for **1** and **2** (600 and 150 MHz, TMS,  $\delta$  ppm)

No.	<b>1</b>				<b>2</b>		
	$\delta_C^a$	$\delta_H$ (J in Hz) <sup>a</sup>	HMBC (H→C) <sup>a</sup>	COSY <sup>a</sup>	$\delta_C^a$	$\delta_H$ (J in Hz) <sup>a</sup>	$\delta_H$ (J in Hz) <sup>b</sup>
1	59.4C				59.6C		
2	198.3C				198.7C		
3	109.3C				109.9C		
4	45.2CH	3.49 (1H, s)	2, 3, 5, 6, 7, 8, 9, $CH_3$ -5		45.8CH	3.55 (1H, s)	3.53 (1H, s)
5	74.8C				74.3C		
6	210.2C				209.8C		
7	38.0CH <sub>2</sub>	a: 1.75 (1H, d, 14.0) b: 2.57 (1H, d, 14.0)	1, 2, 6, 8, 15, 19 1, 2, 4, 6, 8, 15, $CH_3$ -1	7b 7a	33.8CH <sub>2</sub>	a: 2.04 (1H, d, 14.0) b: 2.44 (1H, d, 14.0)	2.14 (1H, d, 13.7) 2.61 (1H, d, 13.7)
8	57.6C				57.0C		
9	166.6C				166.1C		
10	118.5CH	6.41 (1H, d, 14.6)	3, 9, 11, 12	11	118.5CH	6.42 (1H, d, 14.9)	6.20 (1H, d, 14.6)
11	141.8CH	7.12 (1H, dd, 14.6, 10.7)	9	10, 12	141.7CH	7.11 (1H, dd, 14.9, 11.0)	7.21 (1H, dd, 14.6, 11.4)
12	130.9CH	6.32 (1H, dd, 15.1, 10.7)	11, 13	11, 13	130.9CH	6.30 (1H, dd, 15.1, 11.0)	6.33 (1H, dd, 14.6, 11.4)
13	139.1CH	6.21 (1H, dq, 15.1, 6.4)	11, 12	12, 14	139.1CH	6.21 (1H, dq, 15.1, 6.4)	6.16 (1H, dq, 14.6, 6.6)
14	18.7CH <sub>3</sub>	1.84 (3H, d, 6.4)	12, 13	13	18.7CH <sub>3</sub>	1.84 (3H, d, 6.4)	1.88 (3H, d, 6.6)
15	193.5C				192.8C		
16	128.3C				128.5C		
17	145.8CH	6.83 (1H, dd, 2.3, 2.2)	15, 16, 19	19	147.8CH	7.09 (1H, d, 2.3)	7.08 (1H, d, 2.2)
18	66.7CH	5.03 (1H, ddd, 8.3, 3.2, 2.3)	16, 17	18-OH, 19	69.5CH	4.78 (1H, br dd, 5.9, 5.4)	4.87 (1H, m)
19	76.6CH	4.66 (1H, br dd, 5.5, 3.2)	15, 17	17, 18, 19-OH	74.1CH	3.44 (1H, br dd, 6.9, 5.4)	3.47 (1H, d, 8.4)
Me-1	12.1CH <sub>3</sub>	1.10 (3H, s)	1, 2, 6, 7		12.2CH <sub>3</sub>	1.10 (3H, s)	1.21 (3H, s)
Me-5	24.7CH <sub>3</sub>	1.07 (3H, s)	4, 5, 6		25.0CH <sub>3</sub>	1.01 (3H, s)	1.13 (3H, s)
OH-5		6.37 (1H, s)	4, 5, 6			7.29 (1H, s)	
OH-9		13.77 (1H, s)	3, 9			13.68 (1H, s)	
OH-18		5.43 (1H, d, 8.3)	17, 18, 19	18		6.01 (1H, d, 5.9)	
OH-19		5.34 (1H, d, 5.5)	8, 19	19		7.52 (1H, d, 6.9)	

<sup>a</sup> Recorded in DMSO- $d_6$ .

<sup>b</sup> Recorded in CD<sub>3</sub>OD.

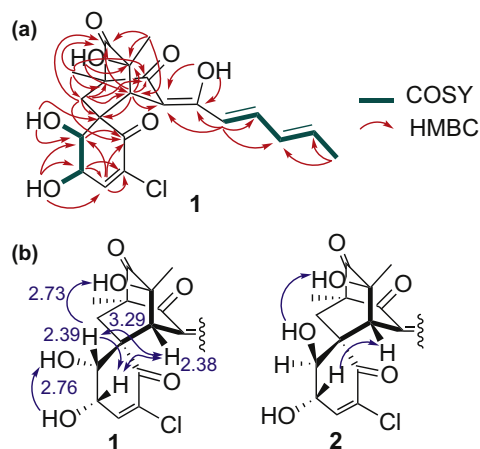


**Fig. 2.** (a) COSY and key HMBC correlations of **1**. (b) Relevant NOE correlations of **1** and **2** and corresponding interatomic distances in the lowest-energy DFT-optimized conformer of **1**.

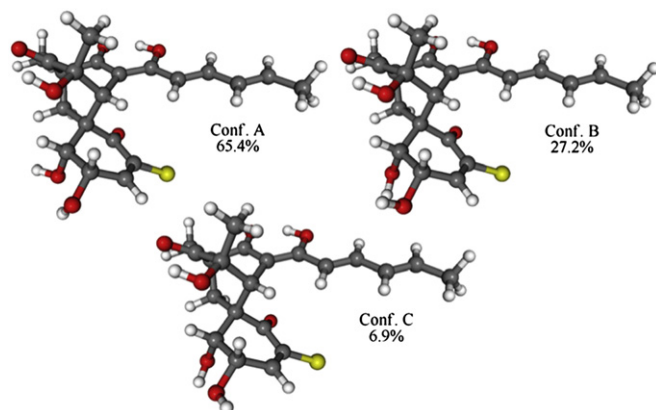


**Fig. 3.** DFT optimized geometries of the three lowest-energy conformers (99.5%) of (1R,4S,5S,8R,18S,19R)-**1**.

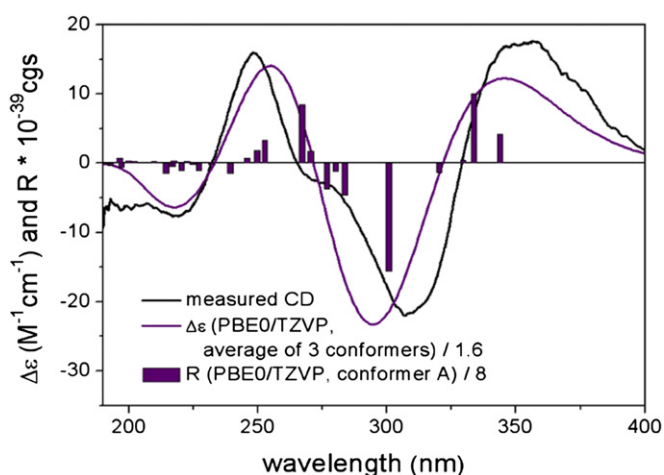


**Fig. 4.** Experimental CD spectrum of **1** in MeOH compared with the PBE0/TZVP Boltzmann-weighted spectrum calculated for the three lowest-energy conformers of the (1R,4S,5S,8R,18S,19R)-enantiomer. Bars indicate the calculated rotatory strengths of conformer A.

An accurate mass analysis of **2** showed the same C<sub>21</sub>H<sub>23</sub>O<sub>7</sub>Cl molecular formula as that of **1**. Its NMR data (Table 1), in particular the COSY and HMBC correlations, revealed that **2** and **1** share the same planar structure implying that they only differ in the

configuration of chiral centers. NOE enhancement of OH-5 was observed upon irradiation of OH-19, which showed that the C-5 hydroxyl group oriented toward the cyclohexenone moiety in **1**. Moreover, NOE effects between H-4 and H-18 was also indicating that H-18 oriented toward the sorbyl side chain. However, the trans relative configuration of H-18 and H-19 was suggested by the 8.4 Hz coupling constant of  $^3J_{18,19}$  measured in CD<sub>3</sub>OD, which was accompanied by chemical shift differences of C-7, C-18, and C-19. The CD spectrum of **2** was nearly identical with that of **1**, which proved that the absolute configuration of the sorbicillin moiety was the same as that of **1**. Therefore compound **2** is the C-19 epimer of **1** and its absolute configuration was determined as (+)-(1R,4S,5S,8R,18S,19S) and named as chloctanspirone B.

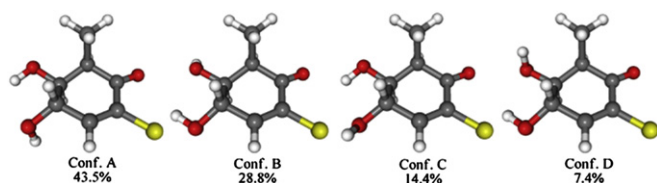
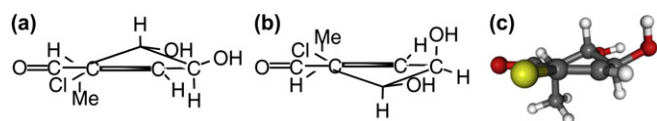
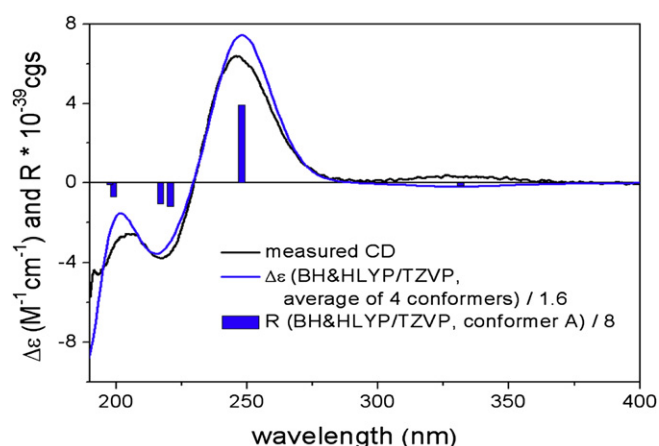
Terrestrol K (**3**) was obtained as an oil. The molecular formula (C<sub>7</sub>H<sub>9</sub>O<sub>3</sub>Cl) was determined by NMR data and its HRESIMS spectrum showing an [M-H]<sup>-</sup> peak at  $m/z$  175.0165. A detailed analysis of the <sup>1</sup>H NMR and <sup>13</sup>C NMR data for **3** indicated the presence of one methyl group, four methines, two quaternary carbons, and two hydroxyl groups (Table 2). The COSY experiment readily established the carbon skeleton from C-3 to C-7 as well as the positions of two hydroxyl groups. Furthermore, the HMBC correlations between H-7 and C-1, between H-3 and C-1, and between H-4 and C-2 completed the planar structure of **3** by the connectivity of C-2 to C-6 via C-1.

The analysis of  $^3J_{H,H}$  coupling constants was used to deduce the relative configuration. The small coupling constant of  $^3J_{3,4}$  (2.3 Hz) indicated that the  $\omega_{H-3,C-3,C-4,H-4}$  dihedral angle is close to 90° with an axial H-4. On the other hand, the large coupling constant measured for  $^3J_{4,5}$  (8.3 Hz) revealed that H-5 was also axial. In addition, the equatorial orientation of H-6 was deduced from the small value of the  $^3J_{5,6}$  (2.3 Hz). Thus the relative configuration of **3** was determined as (4S\*,5S\*,6R\*). The absolute configuration of **3** was established by TDDFT CD calculation. Although quite a number of semiempirical rules were reported to correlate the stereochemistry of cyclohexenone derivatives with characteristic CD bands, the substitution pattern of **3** with chirality centers did not allow a safe configurational assignment.<sup>7,8</sup> Compound **3** showed a positive n- $\pi^*$  band between 370 and 290 nm, a positive  $\pi$ - $\pi^*$  band (I band) at 245 nm, a negative  $\pi$ - $\pi^*$  band at 216 nm (II band made up two  $\pi$ - $\pi^*$  transitions), and a negative  $\pi$ - $\pi$  transition below 200 nm (III band).<sup>7</sup> An MMFF conformational search of **3** followed by DFT optimization afforded four major conformers with 43.5%, 28.8%, 14.4%, and 7.4% populations (Fig. 5). In all the four conformers, H-4 and H-5 were axial, while H-6 had equatorial orientation in accordance with the measured coupling constants. The conformers differed mainly in the orientation of the hydroxyl protons. The cyclohexenone ring had an envelop conformation with C-5 out of the plane (Fig. 6) and the enone chromophore was nearly planar ( $\omega_{O-1,C-1,C-3,C-3}$  torsional angle was close to 180°). The Boltzmann-weighted average of the CD spectra calculated for the four conformers of (4S,5S,6R)-**3** with three functionals reproduced well the  $\pi$ - $\pi^*$  transitions (I–III band). The best agreement was obtained with BH&HLYP/TZVP shown in Fig. 7, which allowed determining the absolute configuration of **3** as (+)-(4S,5S,6R).

Terrestrol L (**4**) was obtained as an oil. The HRESIMS of **4** and NMR data suggested that it was an isomer of **3**, with a molecular formula of C<sub>7</sub>H<sub>9</sub>O<sub>3</sub>Cl. The comparison of the 1D NMR data of **4** (Table 2) with those of **3** afforded the same planar structure as **3**. The NOESY correlations between CH<sub>3</sub>-6 and OH-4, as well as between CH<sub>3</sub>-6 and OH-5, suggested that CH<sub>3</sub>-6 and OH-4 located on the same side of the ring and they are axial, while OH-5 had an equatorial orientation. This was also confirmed by the small  $^3J_{H,H}$  coupling constant of the methine protons measured in CD<sub>3</sub>OD ( $^3J_{5,6}$ =2.9 Hz,  $^3J_{4,5}$ =3.3 Hz). Thus **4** had an all-cis relative configuration, i.e., (4S\*,5R\*,6S\*). The CD spectra of **4** showed a negative n- $\pi^*$  band between 370 and 290 nm and a positive  $\pi$ - $\pi^*$  band at 192 nm (III band), i.e., opposite to those of **3**. This suggested that the

**Table 2**NMR data for **3** and **4** (600 and 150 MHz, TMS,  $\delta$ , ppm)

No.	<b>3</b>					<b>4</b>		
	$\delta_{\text{C}}^{\text{a}}$	$\delta_{\text{H}}$ (J in Hz) <sup>a</sup>	HMBC (H $\rightarrow$ C) <sup>a</sup>	COSY <sup>a</sup>		$\delta_{\text{C}}^{\text{a}}$	$\delta_{\text{H}}$ (J in Hz) <sup>a</sup>	$\delta_{\text{H}}$ (J in Hz) <sup>b</sup>
1	192.6C					193.0C		
2	129.6C					131.2C		
3	148.7CH	7.07 (1H, d, 2.3)	1, 2, 5	4		142.7CH	7.04 (1H, dd, 5.5, 1.4)	6.99 (1H, d, 4.8)
4	72.3CH	4.26 (1H, ddd, 8.3, 6.0, 2.3)	2, 5	4-OH, 3, 5		68.0CH	4.18 (1H, br dd, 6.0, 5.5)	4.31 (1H, dd, 4.8, 3.3)
5	76.5CH	3.32 (1H, ddd, 8.3, 5.5, 2.3)	4	5-OH, 4, 6		74.1CH	3.82 (1H, m)	3.95 (1H, dd, 3.3, 2.9)
6	47.8CH	2.49 (1H, dq, 6.9, 2.3)	1, 4, 5, 7	5, 7		43.4CH	2.99 (1H, dq, 6.9, 2.7)	3.03 (1H, dq, 7.0, 2.9)
7	11.1CH <sub>3</sub>	1.11 (3H, d, 6.9)	1, 5, 6	6		11.1CH <sub>3</sub>	1.09 (3H, d, 6.9)	1.20 (3H, d, 7.0)
4-OH		5.76 (1H, d, 6.0)	3, 4	4			5.72 (1H, d, 6.0)	
5-OH		5.61 (1H, d, 5.5)	5, 6	5			5.43 (1H, d, 4.1)	

<sup>a</sup> Recorded in DMSO-*d*<sub>6</sub>.<sup>b</sup> Recorded in CD<sub>3</sub>OD.**Fig. 5.** DFT optimized geometries of the four lowest-energy conformers (94.1%) of (4S,5S,6R)-**3**. The  $\omega_{\text{O-C1-C3-C5}}$  torsional angle of conformers A–D are  $-178.6^\circ$ ,  $-177.5^\circ$ ,  $-179.7^\circ$ ,  $-179.4^\circ$ , respectively.**Fig. 6.** (a) Schematic representation of the preferred envelop conformation of (4S,5S,6R)-**3** viewed from the direction of the double bond. (b) Preferred envelop conformation of (4S,5R,6S)-**4**. (c) Structure of the lowest-energy conformer of (4S,5S,6R)-**3**.**Fig. 7.** Experimental CD spectrum of **3** compared with the BH&HLYP/TZVP CD spectrum calculated for the four lowest-energy conformers of (4S,5S,6R)-**3**. Bars indicate the calculated rotatory strengths of conformer A (Fig. 5).

envelop conformation (helicity) of the cyclohexenone ring was inverted as shown in Fig. 6b. By introducing the OH-4 and CH<sub>3</sub>-6 in axial and OH-5 in equatorial position into this conformer, the absolute configuration of **4** could be deduced as (+)-(4S,5R,6S).

A possible biosynthetic route to **1** and **2** was proposed (Fig. 8). The methyl groups of the chlorinated precursors **3** and **4** were oxidized and with a subsequent dehydration generated a double bond was produced. By a Diels–Alder reaction, this exocyclic double bond reacted with the diene moiety of the unstable

intermediate (5S)-sorbicillinols,<sup>9</sup> formed from sorbicillin which was also isolated from this fungus, to form the spiro carbon C-8. The absolute configurations of compounds **1** and **2** were in agreement with the precursors (**3** for **2** and **4** for **1**, respectively). The isolation of **3** and **4** indicated that the chlorination step preceded the Diels–Alder reaction.

Most of the reported sorbicillin polymers were produced in the addition of two or three sorbicillin derivatives.<sup>5,10</sup> Natural Diels–Alder products of sorbicillinol with a dienophile not related to the sorbicillinoids were quite rare in nature, and only a few examples have been reported.<sup>6,11</sup> It is the first case that this kind of precursors (**3** and **4**) have been isolated together with the Diels–Alder products (**1** and **2**). To the best of our knowledge, **1** and **2** represent the first natural products containing bicyclo[2.2.2]octane-2-spirocyclohexenone moiety.

The cytotoxicities of **1–4** were preliminarily evaluated in HL-60 and A-549 cells (Table 3) by the MTT method.<sup>4</sup> Compound **1** was active against both cells with IC<sub>50</sub>s 9.2 and 39.7  $\mu\text{M}$ , respectively, while **2** showed weaker activity only against HL-60 cells (IC<sub>50</sub> 37.8  $\mu\text{M}$ ). Interestingly, the inversion of configuration at C-19 affected the activities of **1** and **2** significantly suggesting that although the cyclohexenone moiety was not the pharmacophore (**3** and **4** showed no activities), its stereochemistry influenced the observed activity.

### 3. Experimental section

#### 3.1. General experimental procedures

Optical rotations were obtained on a JASCO P-1020 digital polarimeter. UV spectra were recorded on a Beckman DU<sup>®</sup> 640 spectrophotometer. CD spectra were measured on a J-810 CD spectropolarimeter. IR spectra were recorded on a NICOLET NEXUS 470 spectrophotometer in KBr discs. <sup>1</sup>H, <sup>13</sup>C NMR and DEPT spectra and 2D NMR were recorded on a JEOL JNM-ECP 600 spectrometer and BRUKER AV-400 spectrometer using TMS as an internal standard and chemical shifts were recorded as  $\delta$  values. ESIMS were measured on a Q-TOF ULTIMA GLOBAL GAA076 LC mass spectrometer. Semipreparative HPLC was performed using an ODS column [YMC-pack ODS (A), 10 $\times$ 250 mm, 5  $\mu\text{m}$ , 4 mL/min].

#### 3.2. Fungal material

The fungus *P. terrestris* was isolated from marine sediments collected in Jiaozhou Bay, China. It was identified by Professor C. X. Fang, China Center for Type Culture Collection (identification number: 2004021), and the voucher specimen is preserved in the China Center for Type Culture Collection (patent depositary number: CCTCC M 204077). Working stocks were prepared on Potato Dextrose agar slants stored at 4  $^\circ\text{C}$ .



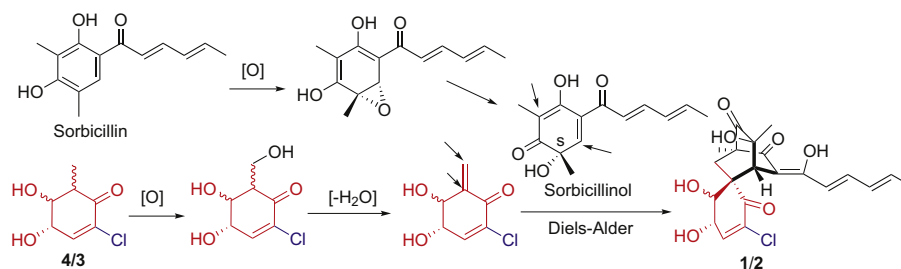


Fig. 8. A possible biosynthetic route to chloctanspirones A (1) and B (2).

Table 3

Cytotoxicities of 1–4 on cancer cell lines

Compound	Cytotoxicity (IC <sub>50</sub> , $\mu$ M)	
	HL-60	A-549
1	9.2	39.7
2	37.8	>100
3	>100	>100
4	>100	>100

### 3.3. Fermentation and extraction

The fungus was cultured under static conditions at 24 °C for 30 days in 200 1000-mL conical flasks containing the liquid medium (300 mL/flask) composed of soytone (0.1%), soluble starch (1.0%), and seawater (60%) as described previously.<sup>4</sup> The fermented whole broth (60 L) in the modified culture condition was filtered through cheese cloth to separate it into supernatant and mycelia. The former was extracted three times with EtOAc to give an EtOAc solution and concentrated under reduced pressure to give a crude extract (20.0 g).

### 3.4. Purification

The crude extract (20.0 g) was purified by a silica gel (200–300 mesh) column packed in petroleum ether. The column was eluted by gradient ratios of petroleum ether–CHCl<sub>3</sub> and then with CHCl<sub>3</sub>–MeOH. The active fraction (Inhibitory rate >50% at a concentration of 100  $\mu$ g/mL) that was eluted with CHCl<sub>3</sub>–MeOH (50:1) was further separated into three subfractions by Sephadex LH-20 using CHCl<sub>3</sub>–MeOH (1:1) as the eluting solvent. Subfraction 1 was further purified by PHPLC (62% MeOH, 4.0 mL/min), to give **1** (13.6 mg) and **2** (13.1 mg). The active fraction eluted with CHCl<sub>3</sub>–MeOH (100:1) was further separated into four subfractions by Sephadex LH-20 using CHCl<sub>3</sub>–MeOH (1:1) as the eluting solvent. Subfraction 4 was subjected to Sephadex LH-20 (CHCl<sub>3</sub>–MeOH, 1:1), then further purified by PHPLC (20% MeOH, 4.0 mL/min) to give **3** (10.3 mg) and **4** (4.9 mg).

**3.4.1. Chloctanspirone A (1).** Yellow powder;  $[\alpha]_D^{25} +304$  (c 0.1, MeOH); ECD (MeOH),  $\lambda$  [nm] ( $\Delta\epsilon$ ), c  $1.18 \times 10^{-3}$ : 356 (17.6), 306 (–22.0), 274sh (–2.8), 248 (15.9), 219 (–7.6); IR (KBr)  $\nu_{\max}$  3419, 1735, 1701, 1612 cm<sup>–1</sup>; UV (MeOH)  $\lambda_{\max}$  nm (log  $\epsilon$ ): 245 (3.67), 359 (3.98); <sup>1</sup>H NMR and <sup>13</sup>C NMR data see Table 1; HRESIMS  $m/z$ : 421.1068 [M–H]<sup>–</sup> (calcd for C<sub>21</sub>H<sub>22</sub>O<sub>7</sub>Cl, 421.1054).

**3.4.2. Chloctanspirone B (2).** Yellow powder;  $[\alpha]_D^{25} +110$  (c 0.1, MeOH); ECD (MeOH),  $\lambda$  [nm] ( $\Delta\epsilon$ ), c  $1.18 \times 10^{-3}$ : 362sh (24.9), 345 (27.6), 306 (–32.1), 273sh (–3.8), 249 (18.9), 221 (–10.0); IR (KBr)  $\nu_{\max}$  3459, 1735, 1700, 1607 cm<sup>–1</sup>; UV (MeOH)  $\lambda_{\max}$  nm (log  $\epsilon$ ): 247 (3.68), 359 (3.97); <sup>1</sup>H NMR and <sup>13</sup>C NMR data see

Table 1; HRESIMS  $m/z$ : 421.1062 [M–H]<sup>–</sup> (calcd for C<sub>21</sub>H<sub>22</sub>O<sub>7</sub>Cl, 421.1054).

**3.4.3. Terrestrol K (3).** Colorless oil;  $[\alpha]_D^{25} +89$  (c 0.1, MeOH); ECD (MeOH),  $\lambda$  [nm] ( $\Delta\epsilon$ ), c  $2.831 \times 10^{-3}$ : 326 (0.4), 245 (6.4), 216 (–3.8), 193 (–4.6); IR (KBr)  $\nu_{\max}$  3360, 1696, 1613 cm<sup>–1</sup>; UV (MeOH)  $\lambda_{\max}$  nm (log  $\epsilon$ ): 240 (3.52); <sup>1</sup>H NMR and <sup>13</sup>C NMR data see Table 2; HRESIMS  $m/z$ : 175.0165 [M–H]<sup>–</sup> (calcd for C<sub>7</sub>H<sub>8</sub>O<sub>3</sub>Cl, 175.0162).

**3.4.4. Terrestrol L (4).** Colorless oil;  $[\alpha]_D^{25} +49$  (c 0.1, MeOH); ECD (MeOH),  $\lambda$  [nm] ( $\Delta\epsilon$ ), c  $2.831 \times 10^{-3}$ : 311 (–0.3), 248 (5.7), 220 (–3.5), 192 (1.0); IR (KBr)  $\nu_{\max}$  3337, 1696, 1612 cm<sup>–1</sup>; UV (MeOH)  $\lambda_{\max}$  nm (log  $\epsilon$ ): 238 (3.54); <sup>1</sup>H NMR and <sup>13</sup>C NMR data see Table 2; HRESIMS  $m/z$ : 175.0159 [M–H]<sup>–</sup> (calcd for C<sub>7</sub>H<sub>8</sub>O<sub>3</sub>Cl, 175.0162).

### 3.5. Biological assays

Cytotoxic activity was evaluated by the MTT method. CDDP (*cis*-diamminedichloroplatinum) was used as positive control. The IC<sub>50</sub> values were obtained using the Bliss method.

### 3.6. Computational section

Conformational searches were carried out by means of the MacroModel 9.7.211<sup>12</sup> software using Merck Molecular Force Field (MMFF) with implicit solvent model for chloroform. In each conformational search the maximum number of steps was set to 30,000. Geometry reoptimizations at B3LYP/6-31G(d) level of theory followed by TDDFT calculations using various functionals (B3LYP, BH&HLYP, PBE0) and TZVP basis set were performed by the Gaussian 03<sup>13</sup> package. Boltzmann distributions were estimated from the ZPVE corrected B3LYP/6-31G(d) energies. CD spectra were generated as the sum of Gaussians<sup>14</sup> with 3000 cm<sup>–1</sup> half-height width (corresponding to ca. 19 nm at 250 nm), using dipole-velocity computed rotational strengths. The MOLEKEL<sup>15</sup> software package was used for visualization of the results.

### Acknowledgements

This work was financially supported by the Chinese National Science Fund (No. 30973627), the Shandong Provincial Natural Science Fund (No. ZR2009CZ016), the Promotive research fund for excellent young and middle-aged scientists of Shandong Province (No. BS2010HZ027), the specialized research fund for the doctoral program of higher education (No. 20100132120026), the Public Projects of State Oceanic Administration (No. 2010418022-3), and the Program for Changjiang Scholars and Innovative Research Team in University (No. IRT0944). The cytotoxicity assays were performed at the Shanghai Institute of Materia Medica, Chinese Academy of Sciences. T.K. thanks the National Office for Research and Technology, Hungarian Scientific Research Fund (NKTH,

K-68429, OTKA, K-81701) TÁMOP 4.2.1./B-09/1/KONV-2010-0007, and János Bolyai Foundation for financial support.

## References and notes

- Blunt, J. W.; Copp, B. R.; Munro, M. H. G.; Northcote, P. T.; Prinsep, M. R. *Nat. Prod. Rep.* **2011**, *28*, 196–268 and previous issues in this series.
- (a) Bode, H. B.; Bethe, B.; Höfs, R.; Zeeck, A. *ChemBioChem* **2002**, *3*, 619–627; (b) Lin, Z.; Zhu, T.; Wei, H.; Zhang, G.; Wang, H.; Gu, Q. *Eur. J. Org. Chem.* **2009**, 3045–3051; (c) Wu, Q. X.; Crews, M. S.; Draskovic, M.; Sohn, J.; Johnson, T. A.; Tenney, K.; Valeriot, F. A.; Yao, X. J.; Bjeldanes, L. F.; Crews, P. *Org. Lett.* **2010**, *12*, 4458–4461.
- (a) Liu, W.; Gu, Q.; Zhu, W.; Cui, C.; Fan, G. *J. Antibiot.* **2005**, *58*, 441–446; (b) Liu, W.; Gu, Q.; Zhu, W.; Cui, C.; Fan, G.; Zhu, T.; Liu, H.; Fang, Y. *Tetrahedron Lett.* **2005**, *46*, 4993–4996; (c) Liu, W.; Gu, Q.; Zhu, W.; Cui, C.; Fan, G. *J. Antibiot.* **2005**, *58*, 621–624.
- Chen, L.; Fang, Y.; Zhu, T.; Gu, Q.; Zhu, W. *J. Nat. Prod.* **2008**, *71*, 66–70.
- Li, D.; Wang, F.; Cai, S.; Zeng, X.; Xiao, X.; Gu, Q.; Zhu, W. *J. Antibiot.* **2007**, *60*, 317–320.
- Neumann, K.; Abdel-Lateff, A.; Wright, A. D.; Kehraus, S.; Krick, A.; König, G. M. *Eur. J. Org. Chem.* **2007**, 2268–2275.
- Gawronski, J. K. *Tetrahedron* **1982**, *38*, 3–26.
- Kirk, D. N. *Tetrahedron* **1986**, *42*, 777–818.
- Abe, N.; Sugimoto, O.; Tanji, K.; Hirota, A. *J. Am. Chem. Soc.* **2000**, *122*, 12606–12607.
- Li, D.; Wang, F.; Xiao, X.; Fang, Y.; Zhu, T.; Gu, Q.; Zhu, W. *Tetrahedron Lett.* **2007**, *48*, 5235–5238.
- (a) Maskey, R. P.; Grün-Wollny, I.; Laatsch, H. *J. Nat. Prod.* **2005**, *68*, 865–870; (b) Bringmann, G.; Lang, G.; Gulder, T.; Tsuruta, H.; Muhlbacher, J.; Maksimenka, K.; Steffens, S.; Schaumann, K.; Stohr, R.; Wiese, J.; Imhoff, J. F.; Perovic-Ottstadt, S.; Boreiko, O.; Muller, W. *Tetrahedron* **2005**, *61*, 7252–7265; (c) Cabrera, G. M.; Butler, M.; Rodriguez, M. A.; Godeas, A.; Haddad, R.; Eberlin, M. N. *J. Nat. Prod.* **2006**, *69*, 1806–1808; (d) Washida, K.; Abe, N.; Sugiyama, Y.; Hirota, A. *Biosci. Biotechnol. Biochem.* **2009**, *73*, 1355–1361.
- MacroModel; Schrödinger LLC: 2009; Portland OR, <http://www.schrodinger.com/Products/macromodel.html>.
- Frisch, M. J.; Trucks, G. W.; Schlegel, H. B.; Scuseria, G. E.; Robb, M. A.; Cheeseman, J. R.; Montgomery, J. A., Jr.; Vreven, T.; Kudin, K. N.; Burant, J. C.; Millam, J. M.; Iyengar, S. S.; Tomasi, J.; Barone, V.; Mennucci, B.; Cossi, M.; Scalmani, G.; Rega, N.; Petersson, G. A.; Nakatsuji, H.; Hada, M.; Ehara, M.; Toyota, K.; Fukuda, R.; Hasegawa, J.; Ishida, M.; Nakajima, T.; Honda, Y.; Kitao, O.; Nakai, H.; Klene, M.; Li, X.; Knox, J. E.; Hratchian, H. P.; Cross, J. B.; Bakken, V.; Adamo, C.; Jaramillo, J.; Gomperts, R.; Stratmann, R. E.; Yazyev, O.; Austin, A. J.; Cammi, R.; Pomelli, C.; Ochterski, J. W.; Ayala, P. Y.; Morokuma, K.; Voth, G. A.; Salvador, P.; Dannenberg, J. J.; Zakrzewski, V. G.; Dapprich, S.; Daniels, A. D.; Strain, M. C.; Farkas, O.; Malick, D. K.; Rabuck, A. D.; Raghavachari, K.; Foresman, J. B.; Ortiz, J. V.; Cui, Q.; Baboul, A. G.; Clifford, S.; Cioslowski, J.; Stefanov, B. B.; Liu, G.; Liashenko, A.; Piskorz, P.; Komaromi, I.; Martin, R. L.; Fox, D. J.; Keith, T.; Al-Laham, M. A.; Peng, C. Y.; Nanayakkara, A.; Challacombe, M.; Gill, P. M. W.; Johnson, B.; Chen, W.; Wong, M. W.; Gonzalez, C.; Pople, J. A. *Gaussian 03, Revision C.02*; Gaussian: Wallingford CT, 2004.
- Stephens, P. J.; Harada, N. *Chirality* **2010**, *22*, 229–233.
- Vareto, U. *MOLEKEL 5.4*; Swiss National Supercomputing Centre: Manno, Switzerland, 2009.